Research Article

# Maternal Pharmacokinetics and Fetal Disposition of (±)-Citalopram during Mouse Pregnancy

Juan C. Velasquez,[‡] Nick Goeden,[‡] Skyla M. Herod,[§] and Alexandre Bonnin*,[†,‡]

[†]Zilkha Neurogenetic Institute, Department of Cell & Neurobiology, Keck School of Medicine of USC, and [‡]USC Neuroscience Graduate Program, University of Southern California, Los Angeles, California 90089, United States

[§]Department of Biology and Chemistry, Azusa Pacific University, Azusa, California 91702, United States

S *Supporting Information*
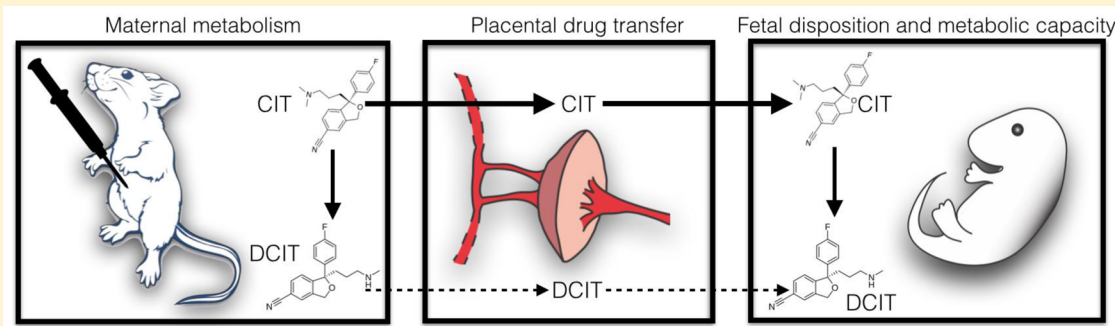
ABSTRACT: While selective-serotonin reuptake inhibitor (SSRI) antidepressants are commonly prescribed in the treatment of depression, their use during pregnancy leads to fetal drug exposures. According to recent reports, such exposures could affect fetal development and long-term offspring health. A central question is how pregnancy-induced physical and physiological changes in mothers, fetuses, and the placenta influence fetal SSRI exposures during gestation. In this study, we examined the effects of gestational stage on the maternal pharmacokinetics and fetal disposition of the SSRI (±)-citalopram (CIT) in a mouse model. We determined the maternal and fetal CIT serum concentration−time profiles following acute maternal administration on gestational days (GD)14 and GD18, as well as the fetal brain drug disposition. The results show that pregnancy affects the pharmacokinetics of CIT and that maternal drug clearance increases as gestation progresses. The data further show that CIT and its primary metabolite desmethylcitalopram (DCIT) readily cross the placenta into the fetal compartment, and fetal exposure to CIT exceeds that of the mother during gestation 2 h after maternal administration. Enzymatic activity assays revealed that fetal drug metabolic capacity develops in late gestation, resulting in elevated circulating and brain concentrations of DCIT at embryonic day (E)18. Fetal exposure to the SSRI CIT in murine pregnancy is therefore influenced by both maternal gestational stage and embryonic development, suggesting potential time-dependent effects on fetal brain development.

KEYWORDS: SSRI, pregnancy, citalopram, fetal brain, placenta

An increasing number of women are prescribed selective serotonin (5-HT) reuptake inhibitor (SSRI) antidepressants to treat depression during pregnancy.[1−7] This pharmacological intervention presents a well-recognized clinical conundrum, namely, the accumulating concerns that developmental abnormalities in the offspring may arise from fetal exposure to maternal depression and to SSRIs.[3,8−11] Few studies have focused on the consequences of prenatal SSRI exposure on fetal neurodevelopment, but recent evidence points to increased risks of autism spectrum disorders and postnatal language learning deficits.[3,12−14] Importantly, developmental outcomes appear to depend on the type of SSRI used and the pregnancy stage of SSRI exposure, suggesting the existence of differences in drug-target interactions and of sensitive time periods for the fetal programming of specific disorders.[3,15] These observations raise questions about the safety of SSRIs during pregnancy and how the factors that affect fetal drug exposures influence short- and long-term offspring health outcomes.

There are highly complex and dynamic maternal physical and physiological changes taking place during pregnancy, a unique condition that also involves the progressive development of the placenta and fetus.[16−20] Pregnancy (and its developmental stage) can thus affect the maternal pharmacokinetics of drug absorption, distribution, metabolism, and elimination, in addition to transplacental transfer and the extent of fetal exposure.[21−28] Therefore, evaluating the impact of pregnancy on these pharmacological factors will provide insight into how they relate to fetal drug exposures potentially leading to different neonatal outcomes.

The maternal, placental, fetal, and genetic factors that determine fetal SSRI exposures in the context of pregnancy remain largely unknown. Studies in humans have largely focused on the maternal pharmacokinetics of SSRIs, showing that maintaining a fixed dose results in low plasma concentrations[29−31] in addition to kinetic changes in drug absorption, distribution, metabolism, and clearance.[18,32−35] The present study characterizes pregnancy-induced changes in the pharmacokinetics of the widely prescribed SSRI (±)-citalopram (CIT) during gestation in mice, and investigates how these influence fetal drug exposure. We first compared the pharmacokinetics of CIT in nonpregnant and pregnant mice at gestational day (GD) 14 and 18. We then investigated the disposition of CIT to the fetus by quantifying placental drug transfer and the extent of fetal exposure following maternal administration. Lastly, we investigated whether the maternal and fetal metabolism of CIT is dependent on gestational age. The data reveal important changes in the maternal and fetal pharmacokinetics of CIT and its major metabolite during development in mice.

■ RESULTS

Pregnancy Affects the Disposition and Pharmacokinetics of CIT. To test whether pregnancy affects CIT pharmacokinetics, we administered a single, fixed dose (FD) of CIT (0.6 mg) to nonpregnant mice and pregnant mice at GD18 (termed GD18$_{FD}$). Blood serum concentrations in both groups showed biexponential decreases overtime from 3.5 min to 3.5 h post administration (Figure 1). Pharmacokinetic
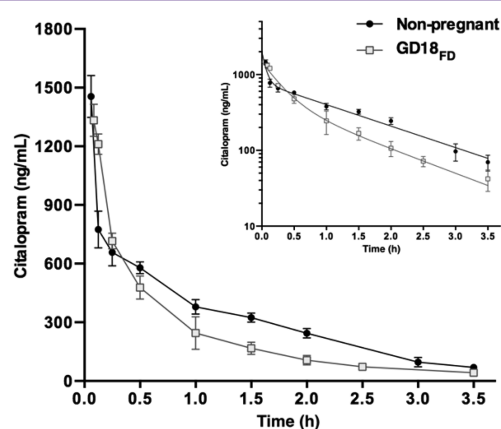

Figure 1. CIT serum concentration−time profiles in pregnant and nonpregnant female mice. A fixed dose (FD) of CIT (0.6 mg) was administered ip to nonpregnant mice (●) and pregnant mice at GD18 (GD18$_{FD}$; □). Mice were sacrificed 3.5 min to 3.5 h following drug administration and CIT serum concentrations were determined by HPLC. Data represent means ± SD (N = 3 mice per time point). The inset (upper right) shows a semilogarithmic plot of serum CIT concentrations over time. Both pregnant and nonpregnant female mice show biexponential decreases in serum CIT concentrations over time.

analysis revealed that blood serum CIT reached higher peak concentrations (C_0) in nonpregnant female mice than in pregnant GD18$_{FD}$ mice (P = 0.0002; Table 1). Consistent with lower serum CIT concentrations measured throughout the 3.5 h time course (Figure 1), a significant 25% reduction in the AUC of serum CIT was observed in GD18$_{FD}$ dams compared to nonpregnant mice [t(4) = 10.97; P = 0.0004; Table 1]. Although time course analyses from both groups showed

Table 1. Comparison of CIT Pharmacokinetics in Nonpregnant and Pregnant (GD18$_{FD}$) Mice[a]

CIT parameter	nonpregnant	GD18$_{FD}$	P value
C_0 (ng/mL)	2050 ± 36	1667 ± 38	p = 0.0002[b]
AUC (ng × h/mL)	1233 ± 39	927 ± 28	p = 0.0004[b]
$t_{1/2}$ (h)	1.06 ± 0.04	0.93 ± 0.06	p = 0.0323[b]
V_D (mL)	29.3 ± 2.3	36.0 ± 2.6	p = 0.0273[b]
C_L (mL × h)	486 ± 9	647 ± 20	p = 0.0002[b]

[a]The CIT serum concentration time-courses were fitted to a two-compartment model to estimate the following pharmacokinetic parameters: C_0, peak concentration, $t_{1/2}$, half-life; AUC, area under the concentration−time curve; V_D, volume of distribution; C_L, clearance. Data are reported as the means ± SD (N = 3 mice per time point). Statistical differences were determined by unpaired two-tailed Student's t tests. [b]Statistically significant differences (P < 0.05) between groups. FD = fixed dose.

similar CIT absorption phases (1.67 vs 1.76; t(4) = 2.16; P = 0.0968; nonpregnant and GD18$_{FD}$, respectively), the distribution rate constant (α) during pregnancy was considerably lower than in nonpregnant mice (t(4) = 95.4; P < 0.0001; Supporting Information Table 1), as reflected by an increase in the volume of distribution (V_D; t(4) = 3.40; P = 0.0273; Table 1). Additionally, the elimination rate constant (β) was higher in pregnant than in nonpregnant mice (t(4) = 5.54; P = 0.0052; Supporting Information Table 1), consistent with the higher clearance (C_L) measured at GD18$_{FD}$ (t(4) = 12.9; P = 0.0002; Table 1). The half-life of CIT measured in pregnant dams was slightly lower than that in nonpregnant female mice (t(4) = 3.22; P = 0.0323; Table 1).

Dose Affects CIT Distribution and Clearance during Pregnancy. The results above indicate that pregnancy affects the pharmacokinetics of CIT in mice. We next investigated whether CIT pharmacokinetics were different in pregnant dams when given a weight-adjusted dose. Pregnant mice receiving a weight adjusted (20 mg/kg of body weight, corresponding on average to 1.17 ± 0.05 mg CIT) dose (GD18) had significantly higher serum C_0 than those administered a fixed, non- weight-adjusted dose (GD18$_{FD}$) (0.6 mg, equivalent to 20 mg/kg dose given to nonpregnant mice) [t(4) = 23.6; P < 0.0001; Table 2]. Serum CIT concentrations were higher at every time point in GD18 compared to GD18$_{FD}$ mice (Figure 2A), consistent with a significant increase in AUC (t(4) = 27.1; P = 0.0004; Table

Table 2. Effect of Weight-Adjusted Dose on Pharmacokinetic Parameters of CIT in Pregnant Mice[a]

CIT parameter	GD18	GD18$_{FD}$	P value
C_0 (ng/mL)	2353 ± 33	1667 ± 38	p < 0.0001[b]
C_{0dn} [(ng/mL/μg]	1.96 ± 0.16	2.57 ± 0.38	p = 0.0648
AUC (ng × h/mL)	2236 ± 79	927 ± 28	p = 0.0004[b]
AUC_{dn} [(ng × h/mL)μg]	1.86 ± 0.20	1.48 ± 0.21	p = 0.0937
$t_{1/2}$ (h)	1.08 ± 0.07	0.93 ± 0.06	p = 0.0599
V_D (mL)	50.9 ± 2.0	36.0 ± 2.6	p = 0.0014[b]
C_L (mL × h)	537 ± 19	647 ± 20	p = 0.0002[b]

[a]The CIT concentration−time profiles were fitted to a two-compartment model to estimate all pharmacokinetic parameters. Dose-normalized (dn) C_0 and AUC were also calculated (C_{0dn}; AUC_{dn}). Data are reported as the means ± SD (N = 3 mice per time point). Statistical differences were determined by an unpaired Student's t test. [b]Indicates statistically significant differences (P < 0.05) between groups. FD = fixed dose.
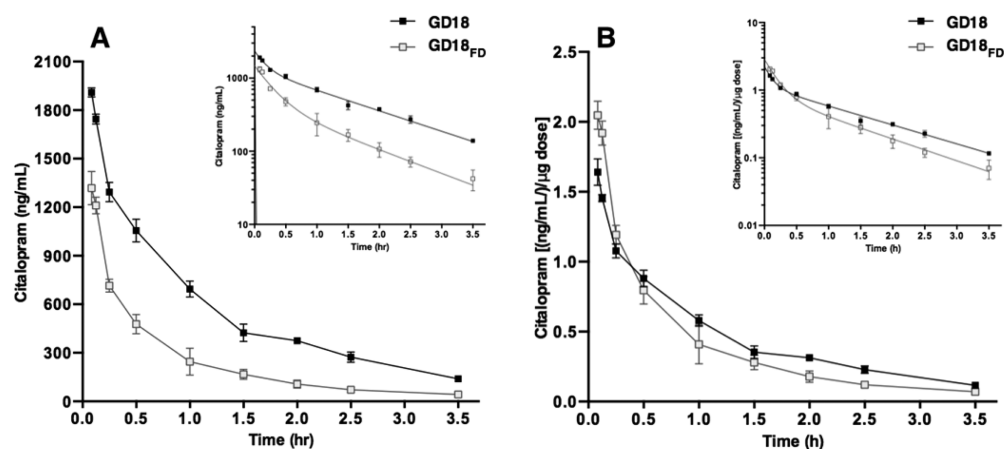
Figure 2. Maternal CIT serum concentration−time profiles in GD18 mice. (A) GD18 Pregnant mice received a weight-adjusted dose of CIT (■; GD18; 20 mg/kg of body weight, ip) or a nonpregnant-equivalent fixed dose (□; GD18$_{FD}$; 0.6 mg, ip). Maternal serum was collected from 3.5 min to 3.5 h after administration, and CIT concentration was measured by HPLC ($N = 3$ dams per time point). (B) Serum concentration−time profiles were normalized to the dose received by dividing the measured CIT serum concentrations by the injected drug amount. Data are shown as the means ± SD ($N = 3$ mice per time point). Insets (upper right) show semilogarithmic plots of the data. FD = fixed dose.
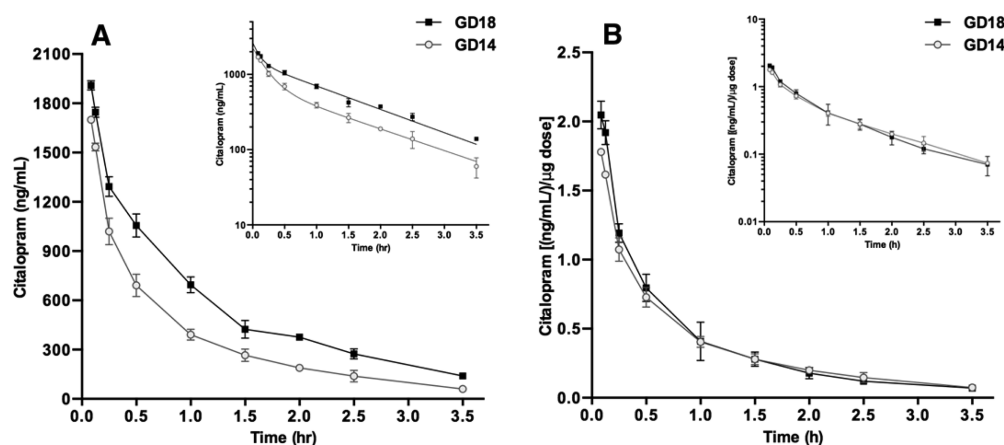
Figure 3. Maternal serum CIT concentration−time profiles in pregnant mice of different gestational stages. (A) Pregnant mice received a weight adjusted CIT dose (20 mg/kg) at GD14 (O) or GD18 (■). Mice were sacrificed 3.5 min to 3.5 h following drug administration and CIT serum concentrations were measured by HPLC. Data represent the means ± SD serum CIT concentration ($N = 3$ mice per time point). The insert (upper right) shows a semilogarithmic plot of the data. (B) Serum concentration−time profiles were normalized to the dose received by dividing the measured CIT serum concentrations by the injected drug amount. Data are shown as the means ± SD ($N = 3$ mice per time point). Inserts (upper right) show semilogarithmic plots of the data. FD = fixed dose.

2). Since the C_0 and AUC estimates are representative of peak CIT concentrations and total drug exposures overtime, we normalized these parameters to the amount of CIT injected. The measured serum CIT concentrations were each divided by injected drug amounts followed by fitting to a two-compartment model. We no longer found significant differences between groups for the above parameters after dose-normalization (C_0; t(4) = 2.56 $P = 0.0648$; AUC; t(4) = 2.30; $P = 0.0937$) (Figure 2B, Table 2). The CIT half-life was unaffected by the dose administered (t(4) = 2.65; $P = 0.0599$; Table 2). When compared to the GD18$_{FD}$ group, an increase in V_D (t(4) = 7.89; $P = 0.0014$; Table 2), as well as a reduction in CIT C_L (t(4) = 12.9; $P = 0.0002$; Table 2) was observed in GD18 mice receiving a weight-adjusted dose. These observations are consistent with significant differences observed in distribution and elimination rate constants (α; t(4) = 5.38; $P = 0.0057$; β; t(4) = 4.65; $P = 0.0097$; Supporting Information Table 1). The differences in $t_{1/2}$, V_D, and C_L between the GD18 and GD18$_{FD}$ groups remained unchanged after dose-normalization.

Pregnancy Stage Affects Disposition and Pharmacokinetics of CIT. The results thus far show that drug dosage and pregnancy affect CIT pharmacokinetics in mice. Significant maternal physical and physiological changes occur progressively throughout pregnancy, therefore we next investigated if CIT pharmacokinetics are affected by pregnancy stage.[16−19] Mice at GD14 and GD18 received a single, weight-adjusted CIT dose (20 mg/kg of body weight). Within each group, maternal serum CIT concentrations decreased over time in a biexponential fashion (Figure 3). The GD18 mice had higher concentrations of CIT at every time point (Figure 3A), consistent with a significantly higher AUC (t(4) = 15.9; $P < 0.0001$; Table 3). Similar differences were observed after dose normalization of these parameters (Table 3). There was a significant increase (22%) in V_D as gestation advanced from GD14 to GD18 (t(4) = 4.97; $P = 0.0076$; Table 3). Drug clearance was also affected by gestational stage, as GD14 mice had significantly higher C_L than GD18 mice (t(4) = 8.58; $P = 0.0010$; Table 3).

Table 3. Gestational Age-Dependent Pharmacokinetics of CIT at GD14 and GD18 in Mice[a]

CIT parameter	GD14	GD18	P value
C_0 (ng/mL)	2278 ± 31	2353 ± 33	$p = 0.0451$[b]
C_{0dn} [(ng/mL)/μg]	2.27 + 0.16	1.96 ± 0.16	$p = 0.0276$[b]
AUC (ng × h/mL)	1388 ± 48	2236 ± 79	$p < 0.0001$[b]
AUC_{dn} [(ng × h/mL)μg]	1.45 ± 0.10	1.86 ± 0.20	$p = 0.0329$[b]
$t_{1/2}$ (h)	1.05 ± 0.03	1.08 ± 0.07	$p = 0.4512$
V_D (mL)	41.7 ± 2.5	50.9 ± 2.0	$p = 0.0076$[b]
C_L (mL × h)	689 ± 15	544 ± 39	$p = 0.0010$[b]

[a]Following CIT administration (20 mg/kg ip), concentration−time profiles were fitted to a two-compartment model to estimate all pharmacokinetic parameters. Dose-normalized (dn) C_0 and AUC were also calculated. Data are reported as the means ± SD ($N = 3$ mice per time point). Statistical differences were determined by an unpaired Student's t test. [b]Indicates statistically significant differences ($P < 0.05$) between groups.

CIT Rapidly Reaches the Fetal Circulation and Brain after Maternal Administration. The effect of pregnancy stage on maternal CIT pharmacokinetics may induce differential exposure of the fetus to the drug over time. Therefore, we measured the kinetics of CIT concentrations in fetal serum and brain at embryonic (E) day 14 and E18 after a single weight-adjusted maternal injection (20 mg/kg, ip). At both embryonic stages, peak fetal serum CIT concentrations were detected within similar time frames (15 min following maternal drug injection (Figure 4A). In addition, fetal serum CIT concentrations decreased biexponentially over time at both E14 and E18. The E18 fetal group had consistently higher serum CIT concentrations than the E14 group (Figure 4A). The fetal/maternal CIT serum concentration ratios (F:M) calculated throughout the 3.5 h period, showed that fetal exposure to CIT exceeded that in mothers 2 h after injection at both gestational ages (F:M > 1), and that F:M were similar between the E14 and E18 groups ($F_{6,24} = 1.42$; $P = 0.2011$; Figure 4B). To test if and how fast the fetal brain is exposed to maternally administered CIT, fetal brain drug concentrations were measured over time and normalized to total protein concentrations. Results show that fetal brain CIT concen-

trations decreased monoexponentially over time at both ages, with the E18 group having consistently higher brain tissue CIT concentrations compared to the E14 group (Figure 4C). In all experiments, fetal sex was determined by SRY genotyping and embryo positions in the uterine horns were recorded. The reported pharmacokinetic measures were not affected by either parameter.

Fetal CIT Disposition Is Independent of Placental/Fetal SERT Expression. Maternally administered CIT rapidly reaches the fetal blood and brain. While passing from the mother to the fetus, the primary binding target for CIT in the placenta is the serotonin transporter (SERT; *Slc6a4*), which is expressed by placental syncytiotrophoblastic cells of fetal origin.[36−41] Placental SERT could act as a local reservoir that limits drug transfer to the fetal compartment. Yet, the influence of binding to placental SERT on the transfer and fetal disposition of CIT is unknown. Here, SERT heterozygous (HET) dams were crossed with SERT HET males to generate SERT wildtype, HET, and knockout (KO) embryos and placentas. To test whether CIT transfer and fetal disposition are influenced by placental/fetal SERT expression, HET dams were injected with CIT (20 mg/kg; ip) at GD18 and CIT concentrations were measured in the serum and brains of fetuses of each genotype. Individual fetal blood and brain collections were performed 1.5 h post maternal drug administration. The HPLC analyses showed no effect of fetal genotype on CIT serum or fetal brain tissue concentrations (serum: $F_{2,12} = 0.34$; $P = 0.7100$; brain: $F_{2,12} = 1.03$; $P = 0.3851$; Figure 5).

Fetal Exposure to DCIT is Dependent on Pregnancy Stage. As uncovered above, fetuses are rapidly exposed to significant concentrations of maternally administered CIT at E14 and E18. In adult mice and humans, CIT is metabolized to the long half-life, SERT-inhibiting metabolite DCIT.[42] During pregnancy, CIT metabolism could therefore result in significant and long-term fetal exposure to this biologically active metabolite. We quantified concentrations of DCIT in maternal and fetal serum samples and brains collected after a single maternal administration of CIT (20 mg/kg; ip). In fetal serum, peak DCIT concentrations were reached faster at E14 (1 h) than E18 (2.5 h) (Figure 6A). However, when taking into
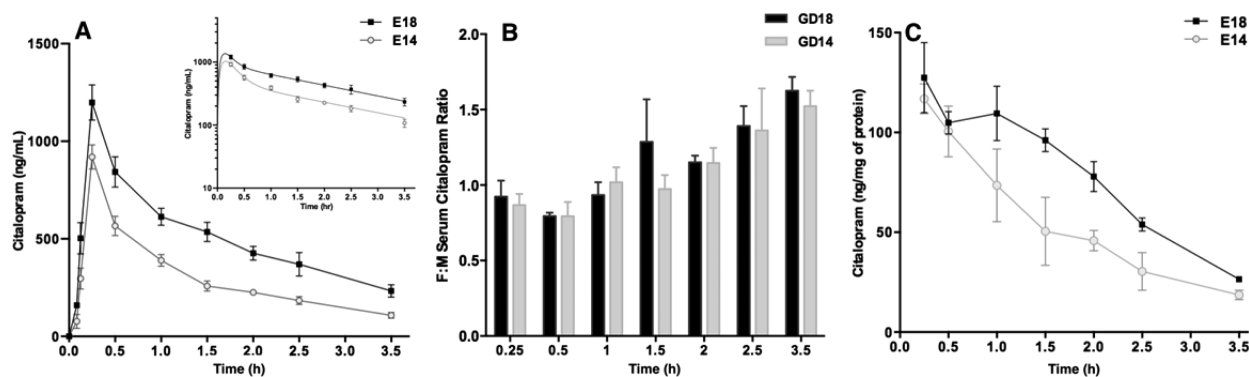

Figure 4. Fetal serum and brain CIT concentration−time profiles during gestation. Pregnant dams at GD14 and GD18 were administered a single ip injection of CIT (20 mg/kg) and CIT concentrations in fetal serum and brain were measured by HPLC. (A) Data show the means ± SD CIT concentration measured in the fetal serum over time from 3.5 min to 3.5 h ($N = 3$ dams per time point, 5−8 pooled fetal samples per dam). The inset (upper right) shows a semilogarithmic plot of the data. (B) Fetal/maternal CIT concentration ratios (F:M) were not significantly different between the GD14 and GD18 groups ($F_{6,24} = 1.42$; $P = 0.2011$; two-way ANOVA followed by Bonferroni adjustment for multiple comparisons). (C) Mean ± SD CIT concentration measured in fetal brain tissue from 15 min to 3.5 h ($N = 3$ dams per time point, 3 fetal brains per dam). The CIT concentrations were normalized to total fetal brain protein concentrations.
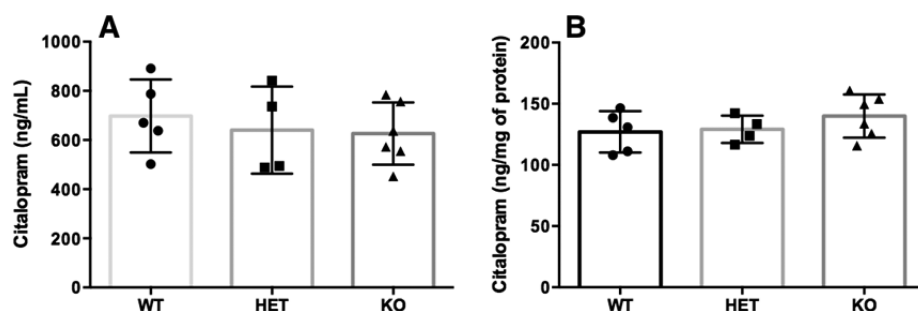
Figure 5. Fetal serum (A) and brain (B) CIT concentrations in wildtype (WT), SERT heterozygous (HET), and SERT knockout (KO) embryos. The SERT HET dams were crossed with SERT HET males and the former received a single CIT injection (20 mg/kg) at GD18. Individual E18 fetal samples were collected 1.5 h postadministration and CIT concentrations were measured by HPLC. Data show the means ± SD CIT concentration (N = 2 dams, 8 total fetal collections per dam). Brain CIT concentrations were normalized to total fetal brain protein.
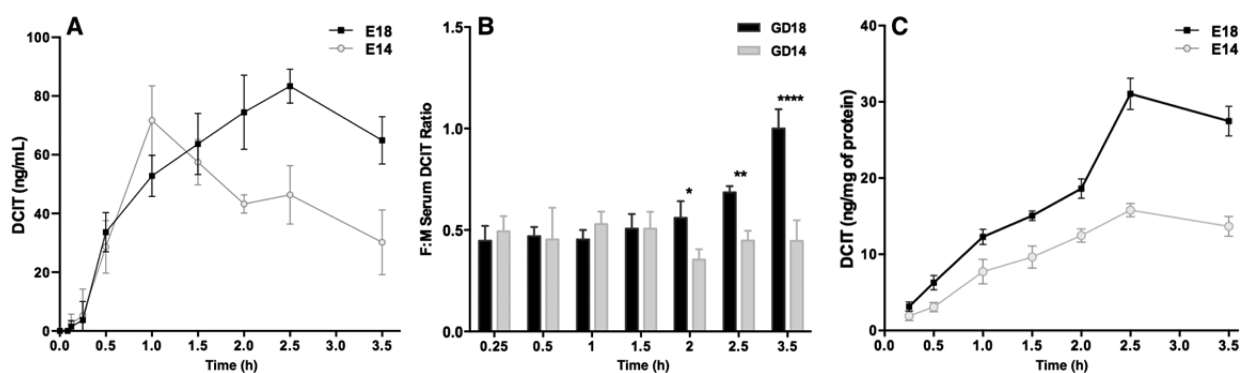

Figure 6. Fetal serum and brain DCIT concentration−time profiles during gestation. Pregnant dams were administered 20 mg/kg CIT ip. The DCIT concentrations in maternal serum, and fetal serum and brain were measured by HPLC. (A) Data show the means ± SD. The DCIT concentrations were measured in fetal serum from 3.5 min to 3.5 h (N = 3 dams per time point, 5−8 pooled fetal samples per dam) at E14 and E18. (B) Fetal/maternal (F:M) DCIT serum concentration ratios. Statistical differences in F:M concentration ratios were analyzed by two-way ANOVA followed by Bonferroni adjustment for multiple comparisons. *P < 0.05; **P < 0.01; ****P < 0.0001. (C) Data show the mean ± SD protein-normalized DCIT concentrations in fetal brain tissue from 15 min to 3.5 h following maternal CIT administration (N = 3 dams per time point, 3 fetal brains per dam).

account DCIT concentrations measured in the maternal serum (Supporting Information Figure 1), the calculated fetal/maternal DCIT serum concentration ratios were higher at E18 vs E14 fetuses 2 h after injection ($F_{6,24}$ = 13.69; P = 0.0166 to <0.0001) (Figure 6B). In the fetal brain, overall DCIT concentrations were higher at E18 than E14, consistent with significantly higher mean AUCs (35.5 ng × h/mL E14 vs 62.8 E18; $F_{2,6}$ = 15.6; P = 0.0159; Figure 6C). Fetal brain DCIT concentrations started to decrease 2.5 h (at E14 and E18) after maternal CIT injection (Figure 6C).

Gestational Age Dependent Changes in CIT Metabolism. Comparatively higher exposure of fetuses to DCIT at E18 than E14 occurred and these differences could result from differential rates of maternal, fetal, and/or placental metabolism between the two ages. To address these possibilities, we first tested if the placenta itself metabolizes CIT. Live E18 placentas were perfused ex vivo with 500 ng/mL CIT continuously infused through the maternal uterine artery. The CIT and DCIT concentrations were measured in the fetal eluates harvested in 10 min intervals through the umbilical vein over a 120 min perfusion period. Here, CIT was detected at every time point in fetal eluates (Figure 7A), indicating that the parent drug readily crosses the live placenta (TI = 0.93 ± 0.55), consistent with the in vivo results. Importantly, DCIT was not detected in the fetal eluate at any time point (Figure 7A). In addition, in vitro assays showed no significant CIT to DCIT metabolic capacity of placental microsomes at any age tested

(Figure 7B). In a separate set of experiments, we measured DCIT transplacental transfer by perfusing live E18 placentas with a maternal solution containing DCIT only (500 ng/mL). The results showed that maternal DCIT readily crossed the placenta (TI = 0.20 ± 0.96) (Figure 7C). These findings indicate that the placenta does not metabolize CIT to DCIT, but allows rapid maternal−fetal DCIT transfer. The maternal compartment is therefore the direct source of DCIT to the fetus.

To test whether maternal CIT metabolism changes during the course of pregnancy, we measured DCIT generation in GD14 and GD18 maternal liver microsomal preparations. The data indicate that the rate of CIT to DCIT metabolism in the maternal liver was similar at GD14 and GD18 (Figure 7D), consistent with in vivo measures showing similar maternal serum DCIT concentrations at both pregnancy stages (AUC; GD18 = 611 ± 66.37 ng × h/mL vs GD14 = 417.5 ± 52.47) [t(2) = 3.234; P = 0.0838] (Supporting Information Figure 1).

These results indicate that variations in maternal CIT metabolism cannot account for the higher DCIT fetal exposure measured in late pregnancy. The remaining possibility was that the rate of CIT to DCIT metabolism in the fetus might be higher at E18 than E14. We compared the rate of DCIT generation from fetal liver microsomes at E14 and E18. There was no measurable DCIT generation from E14 fetal liver microsomes throughout the 2 h incubation period, whereas
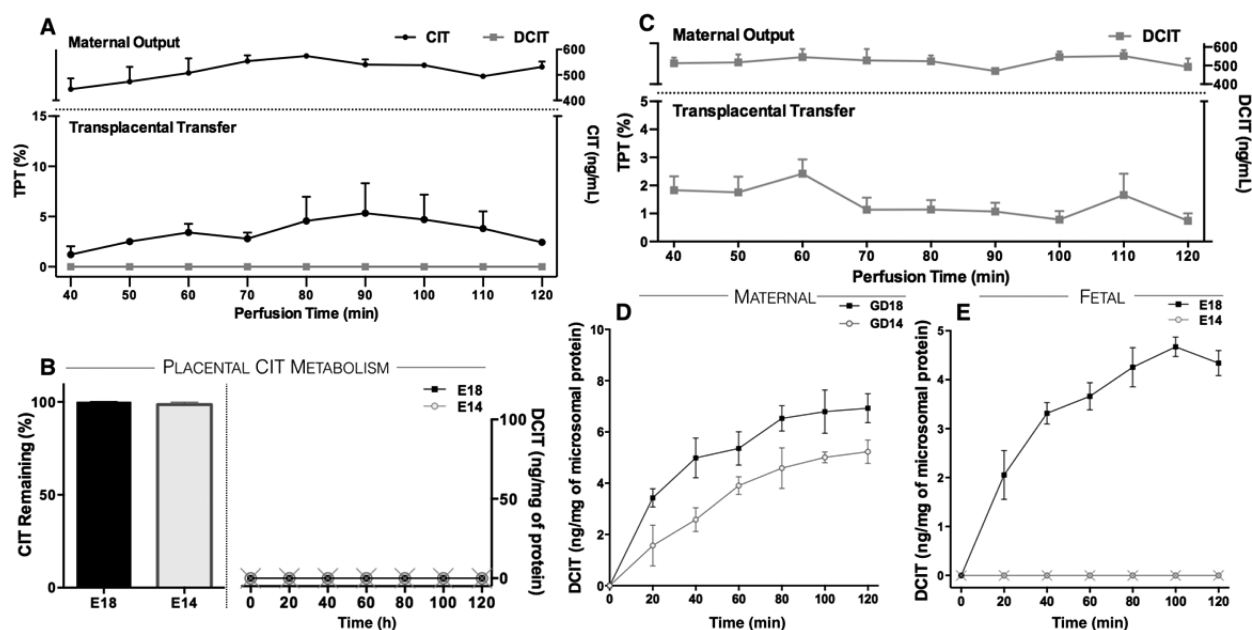
Figure 7. Determination of DCIT sources to the fetal compartment. (A) Placentas were perfused with 500 ng/mL CIT (●) on the maternal side. Perfusion samples were collected every 10 min over a 2 h time period on the maternal (top trace) and fetal (bottom trace) sides and CIT and DCIT (■) concentrations were measured by HPLC (N = 2 independent perfusions). (B) Placental microsomes were isolated at E14 and E18 and incubated with CIT (500 ng/mL). Samples were collected at 20 min intervals over a 2 h period and CIT (left panel; expressed as percent of input) and DCIT (right panel; GD14 (○), GD18 (■) concentrations were measured by HPLC. (C) The GD18 placentas were perfused ex vivo with 500 ng/mL DCIT in the maternal side. Perfusion samples were collected every 10 min over a 2 h time period on the maternal (top) and fetal (bottom) sides and DCIT concentrations were measured by HPLC (N = 3 perfusions). (D) Maternal and (E) fetal liver microsomes were isolated at E14 (○) and E18 (■) and incubated with CIT (500 ng/mL). Data indicate the mean ± SD DCIT concentrations measured by HPLC in samples at 20 min intervals over a 2 h period (N = 2 independent experiments per gestational stage).

there was a significant rate of CIT to DCIT conversion from E18 fetal liver microsomes (Figure 7E).

DISCUSSION

The purpose of the present study was to determine if pregnancy induces stage-dependent changes in the pharmacokinetics and fetal disposition of CIT in mice. We found that the maternal disposition and serum pharmacokinetics of CIT were affected by pregnancy. The C_0 and AUC reductions observed in GD18$_{FD}$ dams are related to the physical changes occurring during pregnancy, namely, the increases in maternal blood volume and total body weight as reflected by a higher V_D (Figure 1, Table 1). Additionally, our results show that drug C_L is increased during pregnancy, which is consistent with observations made for other therapeutic drugs in clinical and preclinical studies.[18,43−45] The increased C_L may also be explained by pregnancy-induced elevation in cardiac output, glomerular filtration rate, and heightened activity of the cytochrome P450 enzymes involved in CIT metabolism during pregnancy (CYP2D6, CYP3A4, CYP2C19).[9,18−20,46] Combined with the fetal metabolic capacity emerging in late pregnancy (Figure 7E), these observations may account for the reduction in CIT terminal half-life in GD18$_{FD}$ compared to nonpregnant female mice. All together, these factors lead to the observed reduction of circulating CIT in the maternal serum at GD18. In the clinical setting, similar decreases in maternal plasma concentrations of CIT or other SSRIs have been suggested to cause reduced therapeutic efficacy of these drugs during pregnancy.[29−34,47]

We next focused on determining whether CIT pharmacokinetics were affected by pregnancy status by adjusting CIT doses

to dam body weights. The weight-adjusted dose administered to GD18 dams (20 mg/kg) was on average twice the amount (1.17 ± 0.05) received by the GD18$_{FD}$ group (maintained at 0.6 mg). Despite this large difference in the amount of CIT administered, we found similar dose-normalized C_0 and AUC parameters between groups (Figure 2, Table 2). However, GD18 dams receiving a CIT dose adjusted to body weight showed a higher V_D and lower C_L than the GD18$_{FD}$ group. Given that mice received CIT at the same gestational stage, these results suggest that a weight-adjusted dosage leads to saturating CIT serum concentrations at GD18. This is also suggested by the significant increase in AUC measured in the GD18 group (141% increase) despite the CIT dose being increased by only 100% (2-fold) over the GD18$_{FD}$ dams. The increase in AUC is not linearly correlated to the administered dose, as expected from systemic drug saturation and consistent with reduced C_L rates.

Similar results were obtained when we investigated the influence of gestational stage on maternal CIT pharmacokinetics with GD14 and GD18 dams receiving CIT adjusted to body weight. We found similar C_0 values following dose-normalization, although AUC remained higher at GD18 (Figure 3, Table 3). In spite of higher serum CIT concentrations at GD18, the terminal half-life was similar at both ages. These results suggest that maternal CIT metabolism is not affected by pregnancy stage. Interestingly, pregnant mice had a lower V_D at GD14 than GD18; this likely results from significant physical changes taking place throughout gestation, in particular the increase of blood volume (estimated to be 8% of body weight and thus corresponding to approximately 3.5 ± 0.1 mL at GD14 vs 4.7 ± 0.2 mL at GD18), and also an increase in overall body lipoprotein content as reflected by

weight gain.[43] In addition, the rapid growth of fetuses from E14 to E18 (average fetal weight increases by 300%) may increase the contribution of the fetal compartment to the apparent V_D.

Changes in CIT maternal pharmacokinetics between GD14 and GD18 may lead to differential exposure of the fetus to the drug over time. Investigation of fetal drug disposition revealed that maternally administered CIT rapidly reaches the fetal circulation and brain (Figure 4). Disposition of CIT in the fetal serum was delayed when compared to the maternal profiles, with fetal serum CIT concentrations peaking 15 min following maternal administration at both E14 and E18. Despite the differences observed in the maternal pharmacokinetics of CIT, fetal to maternal serum concentration ratios were not different between gestational stages, and fetal serum CIT concentrations exceeded maternal concentrations 2 h after maternal administration. These data suggest that there are no major differences in placental CIT permeability between ages and that the kinetics of maternal−fetal transfer through the placenta are faster than efflux back to the maternal compartment.

The SSRI CIT has a high affinity for SERT (K_i = 2.6 nM), which is highly expressed in the placenta, particularly in late gestation (GD18).[44−49] We investigated whether CIT binding to placental SERT could potentially limit transfer to the fetus using heterozygous crossings to generate wildtype, HET, and KO embryos and placentas. Results show that maternal−fetal CIT transport and fetal disposition are completely independent of fetal or placental SERT expression (Figure 5). This result is not unexpected given the multitude of nonspecific drug transporters expressed in the placenta, some of which interact with CIT (e.g., P-gp, BCRP, MDR/ABCB).[54−57] Interestingly, the results suggest that SERT genetic polymorphisms, although studied in clinical populations and correlated to the severity of developmental effects, may not quantitatively affect fetal exposure to CIT during pregnancy.[50,51]

Fetal exposure to biologically active metabolites is another important aspect to consider in the investigation of therapeutic drug use during pregnancy. In humans, SSRIs are metabolized to demethylated forms by cytochrome P450 (CYP) 2D6 and 2C19 enzymes, with large interindividual variation in their respective activities. This leads to important differences in parent drug and metabolite concentrations among individuals. In contrast, rodents are generally assumed to correspond to "extensive-metabolizers" for most drugs,[42,52,53] which constitutes a bias for in vivo pharmacodynamics and drug disposition studies. Additionally, the mean plasma S/R enantiomer ratio of racemic CIT is 0.56 and that of DCIT is 0.7 in patients, indicating stereoselective metabolism of CIT.[54] This is possibly due to a higher affinity of S-CIT and S-DCIT to particular metabolizing isoenzymes, suggesting that the most active enantiomer (S-) is also preferentially metabolized. The primary metabolite of CIT, DCIT, is biologically active and also displays a prolonged half-life.[42] Although the inhibitory constant (K_i) of SERT-mediated 5-HT uptake is less potent than its parent drug (DCIT = 14 nM; CIT = 2.6 nM) it is comparable to that of the commonly used SSRI fluoxetine (K_i = 14 nM).[42] In this light, maternal use of CIT during pregnancy could result in long-term fetal exposure to a potent SERT-inhibiting metabolite, besides the parent drug itself.

Our results show that DCIT reaches the fetal circulation and brain following CIT biotransformation (Figure 6). In vivo observations were consistent with ex vivo placental perfusion studies showing that DCIT crosses the placenta (Figure 7). Furthermore, our data show that F:M ratios of CIT (Figure 4B)

are consistently higher than DCIT (Figure 6B), suggesting that DCIT does not cross the placenta as efficiently as CIT. Ex vivo measures also showed that DCIT is transferred transplacentally ∼2-fold less efficiently than CIT (Figure 7A,C), although different rates of efflux back to the maternal compartment may also contribute to these differences. These observations are consistent with the physicochemical properties of CIT vs DCIT, namely, its higher lipophilicity (CIT partition coefficient = 0.48; DCIT = 0.28), and intermediate protein binding that facilitate membrane permeability of CIT over DCIT.[29,55] Additionally, we did not measure any detectable biotransformation when placentas were infused with CIT or in placental microsomal incubations at E14 and E18 (Figure 7). These results are consistent with previous studies showing an absence of placental expression of CYP isoenzymes involved in CIT metabolism and suggest that maternal drug metabolism and placental drug transport are the major determinants of fetal DCIT exposure.[56−58] Importantly, CIT metabolic capacity was detected in the fetal liver at E18 but not E14 (Figure 7E), leading to higher fetal serum DCIT concentrations at E18 compared to earlier in pregnancy (E14). These results parallel observations made in humans where mRNA and protein expression of CIT metabolizing CYP enzymes were not detected in the human fetal liver until 20 weeks of gestation.[59] The differences in fetal exposure to CIT metabolites between E14 and E18 may thus directly reflect changes in fetal CYP expression.

In summary, we have demonstrated that pregnancy affects the pharmacokinetics of CIT. Our findings indicate that drug metabolism and clearance change in a gestational stage-dependent manner and that fetal metabolism may become a significant contributor to these changes during late gestation. These results suggest that in order to account for significant physical and physiological changes that occur throughout pregnancy and to maintain therapeutic efficacy, the CIT doses administered to pregnant mice may need to be adjusted to the maternal pregnant weight. However, the possibility that a nonweight-adjusted dose of CIT administered to pregnant mice still provides an antidepressant effect remains to be tested. Importantly, although we found no differences in fetal drug disposition between E14 and E18, our data show that fetal CIT serum concentrations exceed maternal concentrations 1.5 to 2 h after maternal administration at both ages (Figure 6B). Combined with elevated DCIT levels resulting from fetal metabolism at E18, results are suggestive of extensive fetal exposures to biologically active compounds during late gestation. The capacity of DCIT for blocking SERT function may have neurodevelopmental consequences. Hence, SERT expression starts around midgestation in the fetal brain, a time when serotonin signaling exerts critical trophic influences, such as the modulation of thalamocortical axons pathfinding.[60−66] In particular, if CIT-mediated inhibition of SERT function in the fetal brain leads to increased extracellular serotonin levels, the consequent increase in serotonin signaling in thalamic neurons is expected to induce a dorso-medial shift in the trajectory of thalamocortical axons as they navigate toward the cortex.[66] The potential impact of CIT and DCIT-mediated inhibition of SERT function on the development of these neuronal pathways is currently the subject of investigation. The results provide novel insights into the pregnancy-specific pharmacokinetics of a common SSRI, and demonstrate the importance of fetal metabolism in overall fetal drug exposure. Although the relevance to human pregnancy will need confirmation, the

data suggest that developmental toxicology studies in mice should not only report maternal–fetal drug transport parameters but also carefully consider the influence of maternal, placental and fetal drug metabolism.

■ METHODS

Animals. Nonpregnant female and timed-pregnant CD-1 mice were obtained from Charles River Laboratories (Wilmington, MA), the latter at GD11 (plug date was considered GD1). The B6.129(Cg)-Slc6a4^{tm1Kpl}/J serotonin transporter knockout (KO) female mice and C57BL/6J male mice were purchased from Jackson Laboratories (Bar Harbor, ME) to generate nonsibling heterozygous (HET) breeder mice, which were then bred to generate wildtype (WT), HET, and knockout (KO) fetal genotypes. All genotyping of serotonin transporter (SERT)-deficient mice was conducted by Laragen, Inc. (Culver City, CA). Mice were age-matched (8–10 weeks of age) and pregnancy stage was confirmed by maternal body weights measured at GD14 and GD18 prior to drug administration, and fetal body weights measured at time of harvesting. The GD14 and GD18 stages of mouse pregnancy (roughly equivalent to the first and second trimesters in humans)[67] take place after the placenta has acquired its definitive structure. These are also periods of active neurogenesis and axonal pathway formation in the fetal brain, processes that are modulated by 5-HT and could therefore be impacted directly by maternal–fetal transfer of SSRIs.[68,69] Additionally, the mouse placenta is functional at these time points, which enabled us to assess potential differences in transplacental drug transfer. All mice were housed in groups of 2–3 dams in standard animal facility cages, maintained under 12h:12h light–dark cycles, and with food and water provided ad libitum. All procedures using mice were approved by the Institutional Animal Care and Use Committee at the University of Southern California and Azusa Pacific University (SERT study) and conformed to NIH guidelines.

Citalopram Administration. Racemic citalopram (CIT) hydrobromide (TCI; C2370) was dissolved in 0.9% saline (BD Biosciences) in a volume of 0.01 mL/g. Nonpregnant and pregnant mice at GD14 and GD18 received a single weight adjusted intraperitoneal (ip) injection of 20 mg/kg of body weight CIT. We chose ip administration to evaluate the acute pharmacokinetic parameters following a single CIT dose at controlled time intervals. The 20 mg/kg dose was selected in order to quantify the pharmacokinetic parameters of the CIT dose most commonly used in neuropharmacological studies and which provided an antidepressant effect in mice.[70–73] The mean drug amount administered to nonpregnant mice (0.6 mg CIT) was also injected to GD18 mice (GD18$_{FD}$). The weight adjustment in the administered dose allowed us to take into account the significant maternal physical changes (i.e., weight gain) that occurs during pregnancy, as pregnant CD-1 mice show an ∼2-fold increase in body weight compared to nonpregnant mice by late gestation (Supporting Information Table 2). Dosage of SSRIs during pregnancy is not usually adjusted to changes in body weight in the clinic.[18,74,75] Therefore, we performed dose maintenance studies where the same CIT amount received by nonpregnant mice was administered to heavier dams in late pregnancy (GD18$_{FD}$).

Following CIT administration (N = 3 dams per time point), animals were euthanized under isofluorane anesthesia (Western Medical Supply) by cervical dislocation followed by cardiac puncture at various time intervals (3.5, 5, 7.5, 15, 30 min; 1, 1.5, 2, 2.5, 3, 3.5 h). Nonpregnant and maternal blood was collected in heparinized tubes (BD Biosciences; 367812) and centrifuged at 2000g for 20 min at 4 °C for serum isolation. The uterus was carefully dissected and the embryos were placed in ice-cold phosphate buffered saline (PBS). Fetal blood was collected through the carotid and jugular vasculature at E18 and through the umbilical cord at E14 (N = 5–8 pooled samples per dam). Fetal blood was centrifuged at 2000g for 10 min at 4 °C for serum isolation. Fetal brain samples at E14 and E18 were also dissected at every time point (N = 3–5 per dam). All samples were flash frozen in liquid nitrogen and stored at −80 °C until analysis.

Ex Vivo Transplacental Transfer of CIT and DCIT. Untreated dams were euthanized as above, and a single placenta from each dam was transferred to a thermostated incubation chamber receiving a flow of oxygenated phosphate-buffered saline (PBS; Mediatech) at 37 °C. The uterine artery (maternal input) was cannulated with a 150 μm diameter catheter, and perfused at 20 μL/min with maternal perfusion media (M199 medium without phenol red (Gibco), 2.9 g/dL bovine serum albumin (Amresco), 20 IU USP/mL Heparin, 7.5 g/L Dextran40, 1 g/L glucose, 2.2 g/L sodium bicarbonate, 100 mg/L L-glutamine (Alfa Aesar), 0.001% fast-green dye (Harleco), pH 7.3; all media components were obtained from Sigma-Aldrich unless noted otherwise) containing 500 ng/mL CIT or its primary metabolite desmethylcitalopram (DCIT; Cerilliant; D-047). The uterine vein was connected to 355 μm inner diameter (I.D.) microrenathane tubing (Braintree Scientific; MRE-033) to collect the maternal output. On the fetal side, the umbilical artery was cannulated with a 105 μm I.D. catheter and perfused at 5 μL/min with medium without drugs (modified from above: 30 g/L Dextran40, 0.5 g/L glucose). The umbilical vein was connected to a 305 μm I.D. microrenathane tubing to collect the fetal output. The eluate was collected on both the maternal and fetal sides at 10 min intervals for 120 min and stored at −80 °C until analysis. The ex vivo placental perfusion system and protocol are detailed in refs 76–78.

CIT Metabolism in Microsomal Preparations. Liver microsomes were prepared from individual nonpregnant and maternal livers (N = 2–4 per group), placentas, and fetal livers at GD/E14 and GD/E18 (N = 10–14 per dam) by ultracentrifugation as previously described.[79] Briefly, tissues were dissected and flash-frozen in liquid nitrogen and stored at −80 °C prior to microsomal isolation. Microsomes were prepared by mincing and cleaning tissues in wash buffer to remove blood (225 mM mannitol, 75 mM sucrose, 30 mM Tris-HCl, pH 7.4) and isolated in homogenization buffer (2 mL per 1 g of tissue) with a Teflon pestle (wash buffer + 0.5% (wt/vol) BSA + 0.1 mM EDTA + Roche complete protease inhibitor (Roche; #04693116001, 1 tablet/10 mL). The crude plasma membrane fraction of the homogenate was obtained by two centrifugation steps at 800g for 5 min (discarding the pellet each time) and an additional centrifugation at 10 000g for 10 min. Microsomal and cytosolic proteins were isolated by centrifugation of the supernatant at 25 000g for 20 min followed by 95 000g for 2.5 h. Microsomal proteins present in the pellet fraction were resuspended in wash buffer and centrifuged at 95 000g for 2.5 h. The pellet containing microsomal proteins was resuspended in 1 mL of wash buffer with protease inhibitor. All buffers and centrifugation steps were carried out at 4 °C. Microsomal protein concentrations were measured using a Bradford Assay Kit (BioRad; #500-0207). The quality of the isolated CYP enzymes was assessed by UV spectrum measures at 450 and 420 nm. A peak shifted from 450 to 420 nm indicated that the CYP had undergone degradation.[80]

The CIT metabolic reactions in placental and liver microsomes were prepared as previously described with some modifications.[81–83] Briefly, reactions contained 0.5 mg/mL microsomal protein and 500 ng/mL CIT in wash buffer. The CIT concentration used encompasses maternal blood serum levels measured 5 to 60 min after 20 mg/kg CIT i.p. injections (see Figures 1–3). After preincubation for 2 min in an incubator shaker set at 37 °C, reactions were initiated by addition of NADPH (Sigma-Aldrich; #N1630) to a final concentration of 0.85 mg/mL (final reaction volume 500 μL). Incubations without NADPH served as negative controls and drug stability throughout the assay was assessed by reactions without liver microsomal proteins. A 25 μL sample was taken from each incubation in 10 min intervals from 0 to 120 min. Reactions were terminated with the addition of 25 μL ice-cold HPLC extraction buffer (see sample preparation for HPLC).

Quantification of CIT and DCIT in Biological Samples. *Sample Preparation for HPLC.* A liquid–liquid extraction was used to prepare samples for analysis as previously described.[78] Samples were thawed on ice and extracted with ice-cold extraction buffer (0.2 M perchloric acid + 500 mM D-mannitol +100 μM EDTA) with isoproterenol as internal standard. Extraction buffer was added to fetal serum and microsomal incubations (1:1 v/v) and to maternal serum samples (1:3 v/v). Brain samples were extracted by addition of buffer

(E14 = 300 μL; E18 = 325 μL) followed by sonication (Qsonica; 35% amplification, 15 s). The samples were kept on ice for 30 min before centrifugation 20 000g for 15 min at 4 °C. The supernatant volume was measured and a 10 μL aliquot was injected per sample for HPLC analysis. The resulting pellets were used to measure protein concentrations in brain samples using a Bradford assay.

Perfusion Sample Preparation. Maternal and fetal perfusion samples were thawed on ice. Individual sample volumes were measured (approximately 200 μL for maternal output samples and 50 μL for fetal output samples). Acetonitrile was added to each sample (1:1 v/v) followed by incubation at room temperature for 10 min. Samples were centrifuged at 5000g for 10 min at room temperature. The supernatant volume was measured and evaporated in a SpeedVac concentrator at room temperature. Evaporated samples were resuspended in extraction buffer to the original sample volume. Following HPLC-FLD analysis, the transplacental transfer percentage (TPT) of each drug and associated metabolite was calculated using the following equation: TPT = $(C_f S_f \times 100)/(C_m S_m)$, where C_f is the concentration in fetal venous outflow, S_f is the fetal flow rate (5 μL/min), C_m is the SSRI concentration in maternal arterial inflow, and S_m is the maternal flow rate (20 μL/min). The transplacental transfer index (TI) (i.e., the ratio of transfer between SSRI and antipyrine, used as internal standard) was calculated by dividing the TPT$_{(SSRI)}$ by the TPT$_{(antipyrine)}$.

HPLC Chromatographic Conditions. The measurement of CIT and DCIT in all samples was carried out by high performance liquid chromatography coupled to a fluorescence detector (HPLC-FLD). The analysis was performed using an Eicom 700 system (Eicom Corporation, Kyoto, Japan) consisting of a Shimatzu RF-20AX fluorescence detector (Shimadzu, Kyoto, Japan), an Eicom 700 Insight autosampler, and Envision integration software. An Eicompak SC-30DS C$_{18}$ reversed-phase column packed with 3 μm silica particles (3.0 mm I.D. × 100 mm) was used as the analytical column. Chromatographic conditions were set as previously described.[78,84] Briefly, 10 μL aliquots of each extracted sample were injected into the column and eluted with a mobile phase consisting of 10 mM KH$_2$PO$_4$/acetonitrile (3:1 v/v; EMD Millipore, AX0145P1) (pH 4.0 adjusted with 1 M phosphoric acid), at a flow rate of 500 μL/min. Detection wavelengths were set at 250 nm (excitation) and 325 nm (emission). The retention times were 7.15 and 7.5 min for DCIT and CIT, respectively. The limit of detection for CIT was 1.5 ng/mL and 500 pg/mL for DCIT.

Pharmacokinetic Analysis of CIT and DCIT. Serum drug concentrations-time profiles were fitted to a two-compartment model described by the following equation: $C(t) = A e^{-\alpha t} + B e^{-\beta t}$ (where $C(t)$ is the serum concentration at time t after dosing, A is the fast exponential term, B is the slow exponential term, α is the distribution rate constant, and β is the elimination rate constant (Supporting Information Table 1)) using the compartmental module of SAAM II software (University of Washington, Seattle, WA). The software-generated system of differential equations was modeled after the in vivo serum data using a two-stage population PK analysis.[85,86] Equation term values were obtained from fitting the original serum CIT concentrations obtained in vivo followed by the introduction of a Bayesian (population) term. Once the data were fit, an additional set of population terms were introduced and fitted into the model until 50 iterations that cycled through the data were reached. This method converged to population parameters that reflected an appropriate fit of the model to the data for each of the groups. The goodness of fit was evaluated using the residual method and visual comparison of the actual serum CIT concentration−time profiles to the estimated curve generated by the model. The volume of distribution (V_D), and rates of elimination, absorption, and transfer between the central and peripheral compartments were calculated by the SAAM II software. Other pharmacokinetic parameters were calculated manually as follows:

half-life:

$$t_{1/2} = \frac{\ln(2)}{\beta}$$

where

$$\beta = \frac{k_{2,1} + k_{1,2} + k_{0,1} - \sqrt{(k_{2,1} + k_{1,2} + k_{0,1})^2 - (4k_{1,2}, k_{0,1})}}{2}$$

and where k_{0-2} are rate constants through the different compartments.

peak concentration:

$$C_{(0)} = \frac{\text{dose}}{V_D}$$

area under the curve:

$$\text{AUC} = \frac{\text{dose}}{V_D k_{0,1}}$$

clearance:

$$(C_L) = \frac{\text{dose}}{\text{AUC}}$$

Dose-normalized (dn) parameters (C_{0dn}, AUC$_{dn}$) were also calculated by dividing the measured serum CIT concentrations by injected drug amounts (E14 = 0.9 ± 0.04; E18 = 1.17 ± 0.05 mg CIT) followed by fitting to a two-compartment model. The biexponential equation terms of the model (Supporting Information Table 1) and the calculated mean ± SD of each pharmacokinetic parameter were transferred to GraphPad Prism software v6.0 (La Jolla, CA) to generate concentration−time profile graphs and to perform statistical analyses.

Statistical Analysis. In order to alleviate any potential litter effect, each data point was obtained from three independent dams for maternal pharmacokinetic analyses, or three fetuses pooled from three independent dams for fetal pharmacokinetics analyses. Differences in pharmacokinetic parameters between any two groups were analyzed for statistical significance with unpaired two-tailed Student's t test. Comparisons between more than two groups or added conditions were analyzed with one-way ANOVA and adjusted for multiple comparisons with the Bonferroni correction. Fetal/maternal drug concentration ratios between E14 and E18 were analyzed using two-way ANOVA and adjusted for multiple comparisons with the Bonferroni correction. All statistically significant differences were set at a level of $P < 0.05$.

■ ASSOCIATED CONTENT

Ⓢ Supporting Information

The Supporting Information is available free of charge on the ACS Publications website at DOI: 10.1021/acschemneuro.5b00287.

> Maternal serum DCIT concentration−time profiles during pregnancy; biexponential equation terms for maternal CIT concentration−time profile models; body weights for adult CD-1 mice (nonpregnant) and pregnant dams at GD14 and GD18 (PDF)

■ AUTHOR INFORMATION

Author Contributions

J.C.V. conducted the experiments, with help from N.G. S.M.H. contributed to the SERT knockout experiments. J.C.V. and A.B. designed the experiments, analyzed data, and wrote the manuscript.

Notes

The authors declare no competing financial interest.

■ REFERENCES

(1) Evans, J., Heron, J., Francomb, H., Oke, S., and Golding, J. (2001) Cohort study of depressed mood during pregnancy and after childbirth. *BMJ. 323*, 257−60.

(2) Deave, T., Heron, J., Evans, J., and Emond, A. (2008) The impact of maternal depression in pregnancy on early child development. *BJOG 115*, 1043−51.

(3) Velasquez, J. C., Goeden, N., and Bonnin, A. (2013) Placental serotonin: implications for the developmental effects of SSRIs and maternal depression. *Front. Cell. Neurosci. 7*, 47.

(4) Belmaker, R. H., and Agam, G. (2008) Major depressive disorder. *N. Engl. J. Med. 358*, 55−68.

(5) Government of Canada, Public Health Agency of Canada. (2005) *Depression in Pregnancy*, Public Health Agency of Canada, Toronto, ON.

(6) Davalos, D. B., Yadon, C. A., and Tregellas, H. C. (2012) Untreated prenatal maternal depression and the potential risks to offspring: a review. *Arch. Womens. Ment. Health 15*, 1−14.

(7) Cooper, W. O., Willy, M. E., Pont, S. J., and Ray, W. A. (2007) Increasing use of antidepressants in pregnancy. *Am. J. Obstet. Gynecol. 196*, 544.e1−5.

(8) Olivier, J. D. A., Akerud, H., Kaihola, H., Pawluski, J. L., Skalkidou, A., Högberg, U., and Sundström-Poromaa, I. (2013) The effects of maternal depression and maternal selective serotonin reuptake inhibitor exposure on offspring. *Front. Cell. Neurosci. 7*, 73.

(9) Shea, A. K., Oberlander, T. F., and Rurak, D. (2012) Fetal serotonin reuptake inhibitor antidepressant exposure: maternal and fetal factors. *Can. J. Psychiatry 57*, 523−9.

(10) Olivier, J. D. A., Åkerud, H., and Sundström Poromaa, I. (2015) Antenatal depression and antidepressants during pregnancy: Unraveling the complex interactions for the offspring. *Eur. J. Pharmacol. 753*, 257−262.

(11) Hanley, G. E., and Oberlander, T. F. (2012) Neurodevelopmental outcomes following prenatal exposure to serotonin reuptake inhibitor antidepressants: a "social teratogen" or moderator of developmental risk? *Birth Defects Res., Part A 94*, 651−9.

(12) Croen, L. a, Grether, J. K., Yoshida, C. K., Odouli, R., and Hendrick, V. (2011) Antidepressant use during pregnancy and childhood autism spectrum disorders. *Arch. Gen. Psychiatry 68*, 1104−12.

(13) Harrington, R. a, Lee, L.-C., Crum, R. M., Zimmerman, A. W., and Hertz-Picciotto, I. (2014) Prenatal SSRI Use and Offspring With Autism Spectrum Disorder or Developmental Delay. *Pediatrics 133*, e1241.

(14) Weikum, W. M. W., Oberlander, T. F., Hensch, T. K., and Werker, J. F. (2012) Prenatal exposure to antidepressants and depressed maternal mood alter trajectory of infant speech perception. *Proc. Natl. Acad. Sci. U. S. A. 109* (Suppl), 17221−7.

(15) Altieri, S. C., Yang, H., O'Brien, H. J., Redwine, H. M., Senturk, D., Hensler, J. G., and Andrews, A. M. (2015) Perinatal vs genetic programming of serotonin states associated with anxiety. *Neuropsychopharmacology 40*, 1456−70.

(16) Loebstein, R., Lalkin, A., and Koren, G. (1997) Pharmacokinetic changes during pregnancy and their clinical relevance. *Clin. Pharmacokinet. 33*, 328−43.

(17) Dawes, M., and Chowienczyk, P. J. (2001) Pharmacokinetics in pregnancy. *Best Pract. Res. Clin. Obstet. Gynaecol. 15*, 819−826.

(18) Anderson, G. D. (2005) Pregnancy-induced changes in pharmacokinetics: a mechanistic-based approach. *Clin. Pharmacokinet. 44*, 989−1008.

(19) Isoherranen, N., and Thummel, K. E. (2013) Drug metabolism and transport during pregnancy: how does drug disposition change during pregnancy and what are the mechanisms that cause such changes? *Drug Metab. Dispos. 41*, 256−62.

(20) Feghali, M. N., and Mattison, D. R. (2011) Clinical therapeutics in pregnancy. *J. Biomed. Biotechnol. 2011*, 783528.

(21) Myllynen, P., Immonen, E., Kummu, M., and Vähäkangas, K. (2009) Developmental expression of drug metabolizing enzymes and transporter proteins in human placenta and fetal tissues. *Expert Opin. Drug Metab. Toxicol. 5*, 1483−99.

(22) Ververs, F. F. T., Voorbij, H. A. M., Zwarts, P., Belitser, S. V., Egberts, T. C. G., Visser, G. H. A., and Schobben, A. F. A. M. (2009) Effect of Cytochrome P450 2D6 Genotype on Maternal Paroxetine Plasma Concentrations during Pregnancy. *Clin. Pharmacokinet. 48*, 677−683.

(23) Evseenko, D., Paxton, J. W., and Keelan, J. a. (2006) Active transport across the human placenta: impact on drug efficacy and toxicity. *Expert Opin. Drug Metab. Toxicol. 2*, 51−69.

(24) Prouillac, C., and Lecoeur, S. (2010) The role of the placenta in fetal exposure to xenobiotics: importance of membrane transporters and human models for transfer studies. *Drug Metab. Dispos. 38*, 1623.

(25) Ploeger, A., Raijmakers, M. E. J., van der Maas, H. L. J., and Galis, F. (2010) The association between autism and errors in early embryogenesis: what is the causal mechanism? *Biol. Psychiatry 67*, 602−7.

(26) Nicoletto, S. F., and Rinaldi, A. (2011) In the womb's shadow. *EMBO Rep. 12*, 30−34.

(27) Pollex, E. K., Feig, D. S., Lubetsky, A., Yip, P. M., and Koren, G. (2010) Insulin Glargine Safety in Pregnancy: A transplacental transfer study. *Diabetes Care 33*, 29−33.

(28) Dilworth, M. R., and Sibley, C. P. (2013) Review: Transport across the placenta of mice and women. *Placenta 34*, S34−S39.

(29) Heikkinen, T., Ekblad, U., Kero, P., Ekblad, S., and Laine, K. (2002) Citalopram in pregnancy and lactation. *Clin. Pharmacol. Ther. 72*, 184−91.

(30) Heikkinen, T., Ekblad, U., Palo, P., and Laine, K. (2003) Pharmacokinetics of fluoxetine and norfluoxetine in pregnancy and lactation. *Clin. Pharmacol. Ther. 73*, 330−337.

(31) Freeman, M. P., Nolan, P. E., Davis, M. F., Anthony, M., Fried, K., Fankhauser, M., Woosley, R. L., and Moreno, F. (2008) Pharmacokinetics of sertraline across pregnancy and postpartum. *J. Clin. Psychopharmacol. 28*, 646−53.

(32) Hostetter, A., Stowe, Z. N., Strader, J. R., McLaughlin, E., and Llewellyn, A. (2000) Dose of selective serotonin uptake inhibitors across pregnancy: clinical implications. *Depression Anxiety 11*, 51−7.

(33) Lattimore, K. A., Donn, S. M., Kaciroti, N., Kemper, A. R., Neal, C. R., and Vazquez, D. M. (2005) Selective serotonin reuptake inhibitor (SSRI) use during pregnancy and effects on the fetus and newborn: a meta-analysis. *J. Perinatol. 25*, 595−604.

(34) Deligiannidis, K. M., Byatt, N., and Freeman, M. P. (2014) Pharmacotherapy for mood disorders in pregnancy: a review of pharmacokinetic changes and clinical recommendations for therapeutic drug monitoring. *J. Clin. Psychopharmacol. 34*, 244−55.

(35) Wadelius, M., Darj, E., Frenne, G., and Rane, A. (1997) Induction of CYP2D6 in pregnancy. *Clin. Pharmacol. Ther. 62*, 400−7.

(36) Bottalico, B., Larsson, I., Brodszki, J., Hernandez-Andrade, E., Casslén, B., Marsál, K., and Hansson, S. R. (2004) Norepinephrine transporter (NET), serotonin transporter (SERT), vesicular monoamine transporter (VMAT2) and organic cation transporters (OCT1, 2 and EMT) in human placenta from pre-eclamptic and normotensive pregnancies. *Placenta 25*, 518−29.

(37) Viau, M., Lafond, J., and Vaillancourt, C. (2009) Expression of placental serotonin transporter and 5-HT 2A receptor in normal and gestational diabetes mellitus pregnancies. *Reprod. BioMed. Online 19*, 207−15.

(38) Ganapathy, V., Ramamoorthy, S., and Leibach, F. (1993) TRANSPORT AND METABOLISM OF MONOAMINES IN THE HUMAN PLACENTA - A Review. *Placenta 14*, 35−51.

(39) Yavarone, M. S., Shuey, D. L., Sadler, T. W., and Lauder, J. M. (1993) Serotonin uptake in the ectoplacental cone and placenta of the mouse. *Placenta 14*, 149−161.

(40) Shearman, L. P. L. P. P., McReynolds, A. M., Zhou, F. C., and Meyer, J. S. (1998) Relationship between [125I]RTI-55-labeled cocaine binding sites and the serotonin transporter in rat placenta. *Am. J. Physiol. 275*, C1621−9.

(41) Verhaagh, S., Barlow, D. P., and Zwart, R. (2001) The extraneuronal monoamine transporter Slc22a3/Orct3 co-localizes with

the Maoa metabolizing enzyme in mouse placenta. *Mech. Dev. 100,* 127−30.

(42) Hiemke, C., and Härtter, S. (2000) Pharmacokinetics of selective serotonin reuptake inhibitors. *Pharmacol. Ther. 85,* 11−28.

(43) Shuster, D. L., Risler, L. J., Liang, C.-K. J., Rice, K. M., Shen, D. D., Hebert, M. F., Thummel, K. E., and Mao, Q. (2014) Maternal-fetal disposition of glyburide in pregnant mice is dependent on gestational age. *J. Pharmacol. Exp. Ther. 350,* 425−34.

(44) Zhou, L., Zhang, Y., Hebert, M. F., Unadkat, J. D., and Mao, Q. (2010) Increased glyburide clearance in the pregnant mouse model. *Drug Metab. Dispos. 38,* 1403−6.

(45) Wadelius, M., Darj, E., Frenne, G., and Rane, A. (1997) Induction of CYP2D6 in pregnancy*. *Clin. Pharmacol. Ther. 62,* 400−407.

(46) Mrazek, D. A., Biernacka, J. M., O'Kane, D. J., Black, J. L., Cunningham, J. M., Drews, M. S., Snyder, K. A., Stevens, S. R., Rush, A. J., and Weinshilboum, R. M. (2011) CYP2C19 variation and citalopram response. *Pharmacogenet. Genomics 21,* 1−9.

(47) Milne, R. J., and Goa, K. L. (1991) Citalopram. A review of its pharmacodynamic and pharmacokinetic properties, and therapeutic potential in depressive illness. *Drugs 41,* 450−77.

(48) Thompson, B. J., Jessen, T., Henry, L. K., Field, J. R., Gamble, K. L., Gresch, P. J., Carneiro, A. M., Horton, R. E., Chisnell, P. J., Belova, Y., McMahon, D. G., Daws, L. C., and Blakely, R. D. (2011) Transgenic elimination of high-affinity antidepressant and cocaine sensitivity in the presynaptic serotonin transporter. *Proc. Natl. Acad. Sci. U. S. A. 108,* 3785−90.

(49) Henry, L. K., Field, J. R., Adkins, E. M., Parnas, M. L., Vaughan, R. a, Zou, M., Newman, A. H., and Blakely, R. D. (2006) Tyr-95 and Ile-172 in transmembrane segments 1 and 3 of human serotonin transporters interact to establish high affinity recognition of antidepressants. *J. Biol. Chem. 281,* 2012−23.

(50) Mrazek, D. A., Rush, A. J., Biernacka, J. M., O'Kane, D. J., Cunningham, J. M., Wieben, E. D., Schaid, D. J., Drews, M. S., Courson, V. L., Snyder, K. A., Black, J. L., and Weinshilboum, R. M. (2009) SLC6A4 variation and citalopram response. *Am. J. Med. Genet., Part B 150B,* 341−51.

(51) Oberlander, T. F., Bonaguro, R. J., Misri, S., Papsdorf, M., Ross, C. J. D., and Simpson, E. M. (2008) Infant serotonin transporter (SLC6A4) promoter genotype is associated with adverse neonatal outcomes after prenatal exposure to serotonin reuptake inhibitor medications. *Mol. Psychiatry 13,* 65−73.

(52) Shuster, D. L., Bammler, T. K., Beyer, R. P., Macdonald, J. W., Tsai, J. M., Farin, F. M., Hebert, M. F., Thummel, K. E., and Mao, Q. (2013) Gestational age-dependent changes in gene expression of metabolic enzymes and transporters in pregnant mice. *Drug Metab. Dispos. 41,* 332−42.

(53) Urquhart, B. L., Tirona, R. G., and Kim, R. B. (2007) Nuclear receptors and the regulation of drug-metabolizing enzymes and drug transporters: implications for interindividual variability in response to drugs. *J. Clin. Pharmacol. 47,* 566−78.

(54) Rochat, B., Amey, M., and Baumann, P. (1995) Analysis of enantiomers of citalopram and its demethylated metabolites in plasma of depressive patients using chiral reverse-phase liquid chromatography. *Ther. Drug Monit. 17,* 273−9.

(55) Heikkinen, T., Ekblad, U., and Laine, K. (2002) Transplacental transfer of citalopram, fluoxetine and their primary demethylated metabolites in isolated perfused human placenta. *BJOG 109,* 1003−8.

(56) Ejiri, N., Katayama, K., and Doi, K. (2005) Induction of cytochrome P450 isozymes by phenobarbital in pregnant rat and fetal livers and placenta. *Exp. Mol. Pathol. 78,* 150−5.

(57) Ejiri, N., Katayama, K. I., Nakayama, H., and Doi, K. (2001) Expression of cytochrome P450 (CYP) isozymes in rat placenta through pregnancy. *Exp. Toxicol. Pathol. 53,* 387−91.

(58) Storvik, M., Huuskonen, P., Pehkonen, P., and Pasanen, M. (2014) The unique characteristics of the placental transcriptome and the hormonal metabolism enzymes in placenta. *Reprod. Toxicol. 47,* 9−14.

(59) Hines, R. N., and McCarver, D. G. (2002) The ontogeny of human drug-metabolizing enzymes: phase I oxidative enzymes. *J. Pharmacol. Exp. Ther. 300,* 355−60.

(60) Lebrand, C., Cases, O., Adelbrecht, C., Doye, A., Alvarez, C., El Mestikawy, S., Seif, I., and Gaspar, P. (1996) Transient uptake and storage of serotonin in developing thalamic neurons. *Neuron 17,* 823−35.

(61) Lebrand, C., Cases, O., Wehrlé, R., Blakely, R. D., Edwards, R. H., and Gaspar, P. (1998) Transient developmental expression of monoamine transporters in the rodent forebrain. *J. Comp. Neurol. 401,* 506−24.

(62) Brüning, G., Liangos, O., and Baumgarten, H. G. (1997) Prenatal development of the serotonin transporter in mouse brain. *Cell Tissue Res. 289,* 211−21.

(63) Brüning, G., and Liangos, O. (1997) Transient expression of the serotonin transporter in the developing mouse thalamocortical system. *Acta Histochem. 99,* 117−21.

(64) Narboux-Nême, N., Pavone, L. M., Avallone, L., Zhuang, X., and Gaspar, P. (2008) Serotonin transporter transgenic (SERTcre) mouse line reveals developmental targets of serotonin specific reuptake inhibitors (SSRIs). *Neuropharmacology 55,* 994−1005.

(65) Bonnin, A., Zhang, L., Blakely, R. D., and Levitt, P. (2012) The SSRI citalopram affects fetal thalamic axon responsiveness to netrin-1 in vitro independently of SERT antagonism. *Neuropsychopharmacology 37,* 1879−84.

(66) Bonnin, A., Torii, M., Wang, L., Rakic, P., and Levitt, P. (2007) Serotonin modulates the response of embryonic thalamocortical axons to netrin-1. *Nat. Neurosci. 10,* 588−97.

(67) Cox, B., Kotlyar, M., Evangelou, A. I., Ignatchenko, V., Ignatchenko, A., Whiteley, K., Jurisica, I., Adamson, S. L., Rossant, J., and Kislinger, T. (2009) Comparative systems biology of human and mouse as a tool to guide the modeling of human placental pathology. *Mol. Syst. Biol. 5,* 279.

(68) Kepser, L.-J., and Homberg, J. R. (2015) The neuro-developmental effects of serotonin: A behavioural perspective. *Behav. Brain Res. 277,* 3−13.

(69) Rossant, J., and Cross, J. C. (2001) Placental development: lessons from mouse mutants. *Nat. Rev. Genet. 2,* 538−48.

(70) El Yacoubi, M., Bouali, S., Popa, D., Naudon, L., Leroux-Nicollet, I., Hamon, M., Costentin, J., Adrien, J., and Vaugeois, J.-M. (2003) Behavioral, neurochemical, and electrophysiological characterization of a genetic mouse model of depression. *Proc. Natl. Acad. Sci. U. S. A. 100,* 6227−32.

(71) Crowley, J. J., Brodkin, E. S., Blendy, J. A., Berrettini, W. H., and Lucki, I. (2006) Pharmacogenomic evaluation of the antidepressant citalopram in the mouse tail suspension test. *Neuropsychopharmacology 31,* 2433−42.

(72) Keeney, A. J., and Hogg, S. (1999) Behavioural consequences of repeated social defeat in the mouse: preliminary evaluation of a potential animal model of depression. *Behav. Pharmacol. 10,* 753−64.

(73) Warner-Schmidt, J. L., Vanover, K. E., Chen, E. Y., Marshall, J. J., and Greengard, P. (2011) Antidepressant effects of selective serotonin reuptake inhibitors (SSRIs) are attenuated by antiinflammatory drugs in mice and humans. *Proc. Natl. Acad. Sci. U. S. A. 108,* 9262−7.

(74) Abel, D. E. (2013) Use of selective serotonin reuptake inhibitors during pregnancy. *Contemp. OB/GYN 58,* 46−54.

(75) Cohen, L. S., Altshuler, L. L., Harlow, B. L., Nonacs, R., Newport, D. J., Viguera, A. C., Suri, R., Burt, V. K., Hendrick, V., Reminick, A. M., Loughead, A., Vitonis, A. F., and Stowe, Z. N. (2006) Relapse of major depression during pregnancy in women who maintain or discontinue antidepressant treatment. *JAMA 295,* 499−507.

(76) Goeden, N., and Bonnin, A. (2012) Ex vivo perfusion of mid-to-late-gestation mouse placenta for maternal-fetal interaction studies during pregnancy. *Nat. Protoc. 8,* 66−74.

(77) Goeden, N., and Bonnin, A. (2014) Ex Vivo Perfusion of the Mouse Placenta for Maternal-Fetal Interaction Studies during Pregnancy. In *The Guide to Investigation of Mouse Pregnancy* (Croy,

B. A., Yamada, A. T., DeMayo, F. J., and Adamson, S. L., Eds.), Elsevier, London.

(78) Velasquez, J. C., and Bonnin, A. (2015) Placental Transport and Metabolism: Implications for the Developmental Effects of Selective Serotonin Reuptake Inhibitors (SSRI) Antidepressants. In *Prenatal and Postnatal Determinants of Brain Development − Recent Studies and Methodological Advances*, 1st ed., Springer Science + Business Media New York, New York.

(79) Suski, J. M., Lebiedzinska, M., Wojtala, A., Duszynski, J., Giorgi, C., Pinton, P., and Wieckowski, M. R. (2014) Isolation of plasma membrane-associated membranes from rat liver. *Nat. Protoc. 9*, 312−22.

(80) Jia, L., Bonaventura, C., Bonaventura, J., and Stamler, J. S. (1996) S-nitrosohaemoglobin: a dynamic activity of blood involved in vascular control. *Nature 380*, 221−6.

(81) Jia, L., and Liu, X. (2007) The conduct of drug metabolism studies considered good practice (II): in vitro experiments. *Curr. Drug Metab. 8*, 822−9.

(82) Volotinen, M., Korjamo, T., Tolonen, A., Turpeinen, M., Pelkonen, O., Hakkola, J., and Mäenpää, J. (2010) Effects of selective serotonin reuptake inhibitors on timolol metabolism in human liver microsomes and cryo-preserved hepatocytes. *Basic Clin. Pharmacol. Toxicol. 106*, 302−9.

(83) Olesen, O. V., and Linnet, K. (1999) Studies on the stereoselective metabolism of citalopram by human liver microsomes and cDNA-expressed cytochrome P450 enzymes. *Pharmacology 59*, 298−309.

(84) Meng, Q. H., and Gauthier, D. (2005) Simultaneous analysis of citalopram and desmethylcitalopram by liquid chromatography with fluorescence detection after solid-phase extraction. *Clin. Biochem. 38*, 282−5.

(85) Heatherington, A. C., Vicini, P., and Golde, H. (1998) A pharmacokinetic/pharmacodynamic comparison of SAAM II and PC/WinNonlin modeling software. *J. Pharm. Sci. 87*, 1255−63.

(86) Finkelstein, Y., Nava-Ocampo, A. A., Schechter, T., Grant, M. D. R., Pierre, E. S., Goldman, R., Walker, S., and Koren, G. (2009) Discrepancies in pharmacokinetic analysis results obtained by using two standard population pharmacokinetics software programs. *Fundam. Clin. Pharmacol. 23*, 53−57.